

MOIRCS Deep Survey. X. Evolution of Quiescent Galaxies as a Function of Stellar Mass at $0.5 < z < 2.5$

Masaru KAJISAWA¹, Takashi ICHIKAWA², Tomohiro YOSHIKAWA³, Toru YAMADA², Masato ONODERA⁴,
Masayuki AKIYAMA², Ichi TANAKA⁵

kajisawa@cosmos.ehime-u.ac.jp

¹*Research Center for Space and Cosmic Evolution, Ehime University, Bunkyo-cho 2-5, Matsuyama 790-8577, Japan*

²*Astronomical Institute, Tohoku University, Aramaki, Aoba, Sendai 980-8578, Japan*

³*Koyama Astronomical Observatory, Kyoto Sangyo University, Motoyama, Kamigamo, Kita-ku, Kyoto 603-8555, Japan*

⁴*Institute for Astronomy, ETH Zurich, Wolfgang-Pauli-strasse 27, 8093 Zurich, Switzerland*

⁵*Subaru Telescope, National Astronomical Observatory of Japan, 650 North Aohoku Place, Hilo, HI 96720, USA*

(Received ; accepted)

Abstract

We study the evolution of quiescent galaxies at $0.5 < z < 2.5$ as a function of stellar mass, using very deep NIR imaging data taken with the Multi-Object Infrared Camera and Spectrograph on the Subaru Telescope in the GOODS-North region. The deep NIR data allow us to construct a stellar mass-limited sample of quiescent galaxies down to $\sim 10^{10} M_{\odot}$ even at $z \sim 2$ for the first time. We selected quiescent galaxies with $\text{age}/\tau > 6$ by performing SED fitting of the multi broad-band photometry from the U to *Spitzer* $5.8\mu\text{m}$ bands with the population synthesis model of Bruzual & Charlot (2003) where exponentially decaying star formation histories are assumed. The number density of quiescent galaxies increases by a factor of ~ 3 from $1.0 < z < 1.5$ to $0.5 < z < 1.0$, and by a factor of ~ 10 from $1.5 < z < 2.5$ to $0.5 < z < 1.0$, while that of star-forming galaxies with $\text{age}/\tau < 4$ increases only by factors of ~ 2 and ~ 3 in the same redshift ranges. At $0.5 < z < 2.5$, the low-mass slope of the stellar mass function of quiescent galaxies is $\alpha \sim 0 - 0.6$, which is significantly flatter than those of star-forming galaxies ($\alpha \sim -1.3 - -1.5$). As a result, the fraction of quiescent galaxies in the overall galaxy population increases with stellar mass in the redshift range. The fraction of quiescent galaxies at $10^{11} - 10^{11.5} M_{\odot}$ increases from $\sim 20 - 30\%$ at $z \sim 2$ to $\sim 40 - 60\%$ at $z \sim 0.75$, while that at $10^{10} - 10^{10.5} M_{\odot}$ increases from $\lesssim 5\%$ to $\sim 15\%$ in the same redshift range. These results could suggest that the quenching of star formation had been more effective in more massive galaxies at $1 \lesssim z \lesssim 2$. Such a mass-dependent quenching could explain the rapid increase of the number density of $\sim M^*$ galaxies relative to lower-mass galaxies at $z \gtrsim 1 - 1.5$.

Key words: galaxies:evolution — galaxies:formation — galaxies:high-redshift

1. Introduction

Determining how stars have been formed in galaxies is crucial for understanding galaxy formation and evolution. In the present universe, it is known that galaxies can be well separated into two populations, namely, passively-evolving galaxies with red colors and star-forming galaxies with blue colors (e.g., Kauffmann et al. 2003; Baldry et al. 2004; Brinchmann et al. 2004). Bimodal color distribution which consists of these two populations has also been observed up to $z \sim 1 - 2$ (e.g., Bell et al. 2004; Weiner et al. 2005; Franzetti et al. 2007; Cirasuolo et al. 2007; Cassata et al. 2008; Williams et al. 2009; Brammer et al. 2009). At $z < 1$, several studies have found that the stellar mass density of passively-evolving galaxies increases by a factor of ~ 2 from $z \sim 1$ to $z \sim 0$, while that of star-forming galaxies evolves only very mildly (e.g., Borch et al. 2006; Faber et al. 2007; Pozzetti et al. 2010; Ilbert et al. 2010). Since passively-evolving galaxies hardly accumulate stellar mass only by star formation, these results suggest that some fraction of star-forming galaxies migrates into the

quiescent population by quenching of star formation (Bell et al. 2004; Bell et al. 2007; Faber et al. 2007). Since recent studies suggest that the star formation rates in star-forming galaxies seem to be simply almost proportional to their stellar mass at least at $z \lesssim 2$ (e.g., Elbaz et al. 2007; Daddi et al. 2007; Pannella et al. 2009; Kajisawa et al. 2010), how the quenching of star formation has occurred in galaxies becomes a key issue to understand the various star formation histories of galaxies.

On the other hand, it is also known from studies of the ‘fossil record’ of present-day galaxies that the star formation histories of galaxies seem to depend strongly on their stellar mass (e.g., Heavens et al. 2004; Jimenez et al. 2005). In the local universe, massive galaxies tend to have redder color and older stellar population, while most low-mass galaxies are young and actively star-forming (Kauffmann et al. 2003; Brinchmann et al. 2004). Since the pioneering work by Cowie et al. (1996), many observational studies at higher redshift have suggested that more massive galaxies have older stellar population even at $z \sim 1$ and formed their stars earlier and more rapidly

than low-mass galaxies (e.g., Brinchmann & Ellis 2000; Juneau et al. 2005; Feulner et al. 2005; Bundy et al. 2006; Vergani et al. 2008). For quiescent galaxies with little star formation, Ilbert et al. (2010) and Pozzetti et al. (2010) reported that the number density of low-mass quiescent galaxies increases more rapidly than massive galaxies from $z \sim 1$ to $z \sim 0$. Recently, Peng et al. (2010) proposed that the mass-dependent quenching mechanism which ceases star formation preferentially for more massive galaxies is needed to explain no evolution of the characteristic mass M^* for star-forming galaxies. On the other hand, the increase of low-mass quiescent galaxies at $z \lesssim 1$ is explained by the environmental effects in their scenario. Since the clustering of both bright and faint quiescent galaxies has been observed to be stronger than star-forming galaxies (e.g., Zehavi et al. 2005; McCracken et al. 2008), massive dark matter halos may play some role in the quenching of star formation. It is important to investigate how the evolution of quiescent galaxies and the quenching of star formation depend on stellar mass at higher redshift, as previous studies of the evolution of the global star formation rate density and stellar mass density in the universe suggest that the cosmic star formation rate has a peak around $z \sim 2$ and that a significant fraction of the stellar mass in the present universe had been formed at $z \sim 1$ – 3 (e.g., Hopkins & Beacom 2006; Wilkins et al. 2008).

At $z \sim 1.5$ – 2 , several studies have found massive quiescent galaxies by spectroscopic observations of red objects (e.g., Cimatti et al. 2004; Saracco et al. 2005; Abraham et al. 2007; Kriek et al. 2006; Kriek et al. 2008; Kriek et al. 2009; Onodera et al. 2010) and by color selection techniques with imaging data (e.g., Daddi et al. 2004; Williams et al. 2009; Ilbert et al. 2010; Cameron et al. 2010) or SED fitting techniques with multi-band photometry (e.g., Grazian et al. 2007; Fontana et al. 2009; Whitaker et al. 2010). Ilbert et al. (2010) reported that the number density of massive quiescent galaxies with $M_{\text{star}} \sim 10^{11} M_{\odot}$ rapidly increases from $z \sim 1.75$ and to $z \sim 1$, while it evolves only mildly at $z \lesssim 1$. Furthermore, Fontana et al. (2009) also found that the quiescent fraction in massive galaxies with $M_{\text{star}} > 7 \times 10^{10} M_{\odot}$ significantly increases between $z \sim 2$ and $z \sim 1$. The low fraction of quiescent galaxies at $z \gtrsim 2$ reflects that there are many active star-forming galaxies which dominates the massive galaxy population (e.g., Papovich et al. 2007; Grazian et al. 2007). Thus $1 < z < 2$ seems to be the formation epoch of these massive quiescent galaxies.

On the other hand, Kajisawa et al. (2009) found that the number density of $\sim M^*$ ($\sim 10^{11} M_{\odot}$) galaxies evolves more strongly than low-mass galaxies at $1 \lesssim z \lesssim 3$. Such mass-dependent evolution of the number density may indicate that the star formation history and/or stellar mass assembly of galaxies already strongly depended on stellar mass at that epoch when most stars seen in the present universe were formed. Therefore it is interesting to investigate the mass-dependence of the evolution of quiescent galaxies up to $z \sim 2$. However, low-mass quiescent galaxies at $z \gtrsim 1$ – 1.5 has not yet been investigated so far. Since quiescent galaxies with relatively old stellar population tend

to have high stellar mass-to-luminosity (M/L) ratios, the observed fluxes of quiescent galaxies with a given stellar mass become relatively faint (e.g., Fontana et al. 2003). In order to sample low-mass quiescent galaxies with high completeness, very deep near-infrared (NIR) data are required (e.g., Kajisawa & Yamada 2006).

In this paper, we study the evolution of quiescent galaxies at $0.5 < z < 2.5$ as a function of stellar mass using very deep NIR data from MOIRCS Deep Survey (MODS, Kajisawa et al. 2006; Ichikawa et al. 2007). The MODS data reach ~ 23 – 24 Vega magnitude (~ 25 – 26 AB magnitude) in the K_s band, and they allow us to construct a stellar mass limited sample of quiescent galaxies down to $\sim 10^{10} M_{\odot}$ even at $z \sim 2$. Section 2 describes the observational data and the procedures of source detection and photometry. Details of the SED fitting analysis of the detected objects are given in Section 3. In Section 4, we use the results of the SED fitting to select quiescent galaxies and construct a stellar mass-limited quiescent sample. We show the evolution of the number density and fraction of quiescent galaxies as a function of stellar mass in Section 5. In Section 6, we compare the results with previous studies and discuss their implications. A summary is presented in Section 7.

We use a cosmology with $H_0 = 70 \text{ km s}^{-1} \text{ Mpc}^{-1}$, $\Omega_m = 0.3$ and $\Omega_{\Lambda} = 0.7$. The Vega-referred magnitude system is used throughout this paper, unless stated otherwise.

2. Observational Data and Photometry

We use the K_s -selected sample of the MODS in the GOODS-North region (Kajisawa et al. 2009, hereafter K09), which is based on our deep JHK_s -bands imaging data taken with MOIRCS (Suzuki et al. 2008) on the Subaru telescope. Four MOIRCS pointings cover $\sim 70\%$ of the GOODS-North region ($\sim 103.3 \text{ arcmin}^2$, hereafter referred as “wide” field) and the data reach $J = 24.2$, $H = 23.1$, $K = 23.1$ (5σ , Vega magnitude). One of the four pointings is the ultra-deep field of the MODS ($\sim 28.2 \text{ arcmin}^2$, hereafter “deep” field), where the data reach $J = 25.1$, $H = 23.7$, $K = 24.1$. A full description of the observations, reduction, and quality of the data is presented in a separate paper (Kajisawa et al. 2011).

The source detection was performed in the K_s -band image using the SExtractor image analysis package (Bertin & Arnouts 1996). At first, we limited the samples to $K_s < 23$ and $K_s < 24$ for the wide and deep fields, where the detection completeness for point sources is more than 90% (Kajisawa et al. 2011). Then we measured the optical-to-MIR SEDs of the sample objects, using the publicly available multi-wavelength data in the GOODS field, namely KPNO/MOSAIC (U band, Capak et al. 2004), *Hubble Space Telescope*/Advanced Camera for Surveys (*HST*/ACS; B , V , i , z bands, version 2.0 data; M. Giavalisco et al. 2010, in preparation; Giavalisco et al. 2004) and *Spitzer*/IRAC ($3.6\mu\text{m}$, $4.5\mu\text{m}$, $5.8\mu\text{m}$, DR1 and DR2; M. Dickinson et al. 2010, in preparation), as well as the MOIRCS J - and H -bands images. Details of the multi-band aperture photometry are presented in

Kajisawa et al. (2011). Following K09, we used objects which are detected above 2σ level in more than two other bands in addition to the 5σ detection in the K_s -band, because it is difficult to estimate the photometric redshift and stellar mass of those detected only in one or two bands. The number of those excluded by this criterion is negligible (21/6402 and 42/3203 for the wide and deep fields, respectively).

We also used public *Spitzer*/MIPS $24\mu\text{m}$ data in the GOODS-North (DR1+, M. Dickinson et al., in preparation) to measure $24\mu\text{m}$ fluxes of the sample galaxies. The IRAF/DAOPHOT package (Stetson 1987) was used for the photometry to deal with many blended sources on the image properly. The DAOPHOT software fitted blended sources in a crowded region simultaneously with the PSF of the image. We used the source positions in the MOIRCS K_s -band image as a prior for the centers of the fitted PSFs in the photometry. For most objects, for which the residual of the fitting is negligible, the 5σ limiting flux is $\sim 20 \mu\text{Jy}$. Details of the photometry on the MIPS image and the error estimate are described in Kajisawa et al. (2010) and Kajisawa et al. (2011).

3. SED fitting analysis

K09 estimated the redshift and stellar mass of the K_s -selected galaxies mentioned above and constructed a stellar mass-limited sample to study the evolution of the stellar mass function. We here use the same photometric redshift as in K09 and carry out a similar SED fitting of the multi-band photometry where the grid of model parameters is slightly changed from that in K09 in order to estimate age and star-formation time scale τ (see below) optimally for the selection of quiescent galaxies.

In K09, we show the photometric redshifts agree well with spectroscopic redshifts (Figure 1 in K09). If available, we adopted spectroscopic redshifts from the literature (Cohen et al. 2000; Cohen 2001; Dawson et al. 2001; Wirth et al. 2004; Cowie et al. 2004; Treu et al. 2005; Reddy et al. 2006; Barger et al. 2008; Yoshikawa et al. 2010), and performed the SED fitting fixing the redshift to each spectroscopic value for these galaxies.

We performed the SED fitting of the multi-band photometry (*UBVizJHK*, $3.6\mu\text{m}$, $4.5\mu\text{m}$, and $5.8\mu\text{m}$) with a population synthesis model. We adopted the GALAXEV population synthesis model (Bruzual & Charlot 2003) for direct comparison with previous studies (e.g., Grazian et al. 2007; Fontana et al. 2009). In the model, we assumed exponentially decaying star formation histories with the decaying timescale τ ranging between 0.1 and 100 Gyr. We used Calzetti extinction law (Calzetti et al. 2000) in the range of $E(B - V) = 0.0$ -1.0. Metallicity is changed from 1/50 to 1 solar metallicity. The model age is changed from 50 Myr to the age of the universe at the observed redshifts. We used 18 grid of τ and 60 grid of age (smaller number of grid at higher redshift depending on the age of the universe), which are roughly equally spaced on a logarithmic scale and are slightly finer than those used in K09 to select quiescent galaxies by a criterion with age/τ

(see the next section). We assume Salpeter IMF (Salpeter 1955) with lower and upper mass limits of 0.1 and $100 M_\odot$ for easy comparison with the results in other studies. If we assume the Chabrier-like IMF (Chabrier 2003), the stellar mass is reduced by a factor of ~ 1.8 . The redshifts mentioned above and stellar M/L ratios from the best-fit templates were used to calculate the stellar mass. The estimated stellar mass is reasonably consistent with that in K09, and the slight change in the grid of the model parameters does not affect the estimate of the stellar mass. The uncertainty of the stellar mass is estimated taking into account of the photometric redshift error for those without spectroscopic redshift, and is discussed in detail in K09. In the next section, we will discuss the effect of the stellar mass error on the sample selection.

4. Sample selection

4.1. Selection of quiescent galaxies

Taking advantages of the deep MOIRCS *JHK_s*-bands photometry and the wide wavelength coverage of the multi-wavelength ancillary data of the GOODS, we used the results of the SED fitting described in the previous section to select quiescent galaxies. Several studies have used the SED fitting technique for the selection of quiescent galaxies (Zucca et al. 2006; Arnouts et al. 2007; Grazian et al. 2007; Salimbeni et al. 2008; Fontana et al. 2009). Following Fontana et al. (2009) and Grazian et al. (2007), we use the criterion with age/τ , assuming $\text{SFR} \propto \exp(-\text{age}/\tau)$ in the SED fitting with the GALAXEV model. In this study, we adopt $\text{age}/\tau > 6$ as in Fontana et al. (2009), which roughly corresponds to $\text{SFR}/M_{\text{star}} \lesssim 10^{-11} \text{ yr}^{-1}$ for relatively small τ values (Fontana et al. 2009). It should be noted that our lower limit of $\tau \geq 0.1$ Gyr mentioned in the previous section leads to a lower limit of age > 0.6 Gyr for galaxies with $\text{age}/\tau > 6$. The upper panels of Figure 1 show the distribution of age/τ as a function of stellar mass for galaxies at $0.5 < z < 1.0$, $1.0 < z < 1.5$, and $1.5 < z < 2.5$. Thick dashed line shows the criterion of $\text{age}/\tau = 6$ and thin dashed lines represent $\text{age}/\tau = 5$ and 4. The MIPS $24\mu\text{m}$ sources ($\gtrsim 20\mu\text{Jy}$) are also shown in the figure. The mid-infrared detection indicates dust enshrouded star formation (or AGN activity). It is seen that at $\text{age}/\tau \sim 4$ -5, many galaxies are detected on the MIPS $24\mu\text{m}$ image, especially at $M_{\text{star}} \gtrsim 10^{10.5} M_\odot$, while there are only a small number of $24\mu\text{m}$ sources at $\text{age}/\tau > 6$. The criterion of $\text{age}/\tau > 5$ or 4 could lead to the contamination of the quiescent sample with objects with some star-forming activities. Therefore we use the criterion of $\text{age}/\tau > 6$ in this paper, although we will check the results with the criteria of $\text{age}/\tau > 5$ and 4 in Section 6.1. For the same reason, we excluded the MIPS $24\mu\text{m}$ sources with $\text{age}/\tau > 6$ from the quiescent sample as in Fontana et al. (2009). There are 9, 2, and 3 such $24\mu\text{m}$ sources with $\text{age}/\tau > 6$ at $0.5 < z < 1.0$, $1.0 < z < 1.5$, and $1.5 < z < 2.5$, respectively. The $24\mu\text{m}$ fluxes of these objects could be powered by AGN (e.g., Nardini et al. 2008). We show hard X-ray sources from the Chandra Deep Field North catalog (Alexander et al.

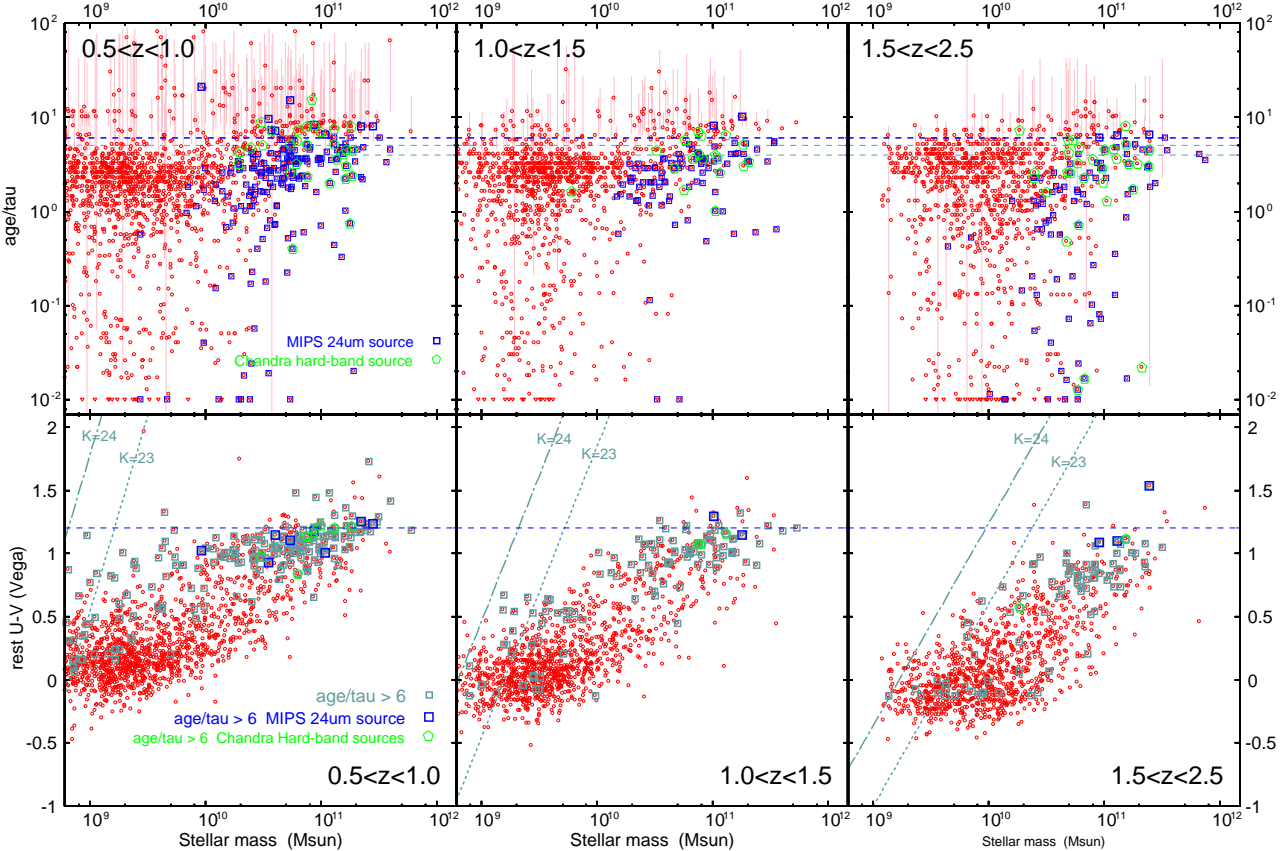


Fig. 1. top: age/τ vs. stellar mass for K_s -selected galaxies in the MODS field in each redshift bin. The uncertainty of age/τ is shown as errorbars for galaxies with $\text{age}/\tau > 6$. Errors in age/τ also include the photometric redshift error for those with no spectroscopic identification. Blue open squares represent objects detected in the MIPS 24 μm image with $S/N > 5$ ($f_{24\mu\text{m}} \gtrsim 20 \mu\text{Jy}$). The MIPS 24 μm sources with $\text{age}/\tau > 6$ are shown as large blue squares. Pentagons show Chandra hard-band sources from the CDF-North catalog (Alexander et al. 2003). Thick dashed line shows the criterion of $\text{age}/\tau = 6$ for quiescent galaxies and thin dashed lines represent $\text{age}/\tau = 5$ and 4. **bottom:** rest-frame $U - V$ color vs. stellar mass for the same K_s -selected galaxies. Gray open squares show galaxies with $\text{age}/\tau > 6$ in the top panels. Blue larger squares and green pentagons show the MIPS 24 μm and Chandra hard-band sources with $\text{age}/\tau > 6$, respectively. Horizontal dashed line represents $\text{rest } U - V = 1.2$. Short-dashed and dashed-dotted lines represent the K_s -band magnitude limit for the wide ($K_s = 23$) and deep ($K_s = 24$) fields, respectively (see text for details).

2003) in Figure 1, and only one of these 24 μm sources with $\text{age}/\tau > 6$ is significantly detected in the hard X-ray data. We also found that the other 13 24 μm sources have the 1.6 μm bump in their near- to mid-infrared SEDs and do not show power-law SEDs. Therefore most of 24 μm sources with $\text{age}/\tau > 6$ are considered to be star-forming galaxies, and we excluded all these 24 μm sources from the quiescent sample as objects with relatively active star formation.

4.2. Limiting stellar mass for quiescent galaxies

The K_s -band magnitude-limited sample does not have a sharp limit in stellar mass even at a fixed redshift, because the stellar M/L ratio at the observed K_s band varies with different stellar populations (e.g., Kajisawa & Yamada 2006; K09). K09 investigated how the K_s -band magnitude limit affects the stellar mass distribution of the sample by using the distribution of the rest-frame $U - V$ color, which reflects the stellar M/L ratio well, as a function of stellar mass (Figure 3 in K09). We here use the similar method to determine the limiting stellar mass for

quiescent galaxies. The bottom panels of Figure 1 show the rest-frame $U - V$ color vs. stellar mass for the K_s -selected galaxies. Quiescent galaxies selected by $\text{age}/\tau > 6$ in the previous section are shown as gray squares. The K_s -band magnitude limits for the wide ($K_s = 23$) and deep ($K_s = 24$) fields are shown as Short-dashed and dashed-dotted lines, respectively. All objects with stellar mass larger than the line at a fixed $U - V$ color (on the right side of the line in the figure) are brighter than the magnitude limit. We used the GALAXEV model with various star formation histories to calculate the line (see K09 for details). The slope of the lines represents that galaxies with redder $U - V$ colors tend to have higher stellar M/L ratios and that at a fixed K_s -band flux (luminosity), the limiting stellar mass for red galaxies is systematically higher than that for blue galaxies.

In the figure, quiescent galaxies with $\text{age}/\tau > 6$ tend to have red $U - V$ colors, typically $U - V \gtrsim 0.8$, especially at $M_{\text{star}} \gtrsim 10^{10} M_{\odot}$, and form the well-known red sequence. It is seen that the color distribution of the qui-

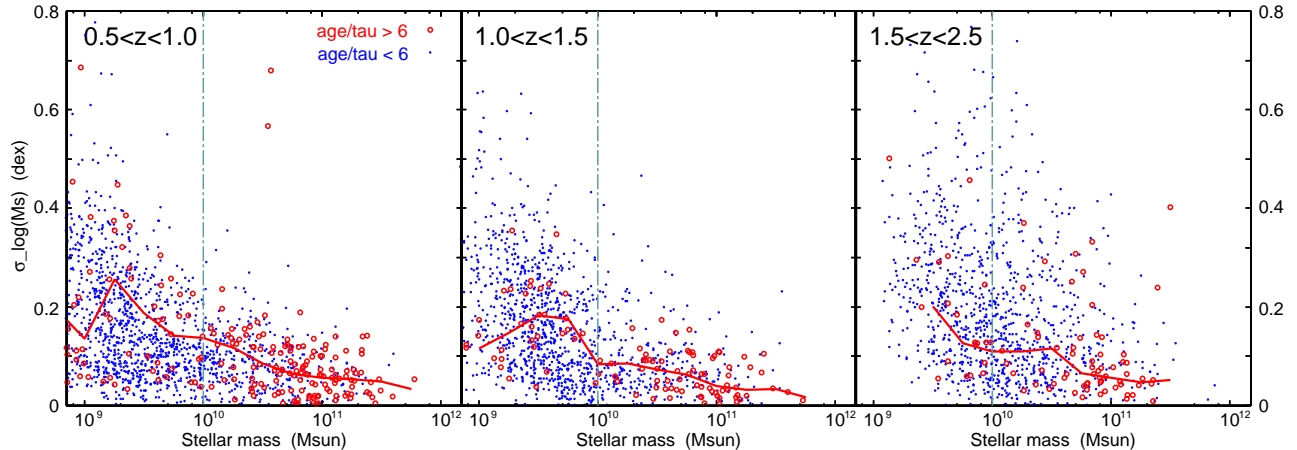


Fig. 2. Uncertainty of the estimated stellar mass as a function of stellar mass in each redshift bin. Red circles show quiescent galaxies with $\text{age}/\tau > 6$ and blue dots represent those with $\text{age}/\tau < 6$. Solid line shows the median values at each stellar mass for quiescent galaxies. Vertical dashed-dotted line represents the limiting stellar mass for the quiescent sample. For objects without spectroscopic redshift, the photometric redshift error is taken into account in the estimate of the stellar mass uncertainty.

escent galaxies shifts to bluer with redshift. If we select galaxies with $U - V > 0.8$, $U - V > 0.7$, and $U - V > 0.6$ as the red sequence population at $0.5 < z < 1.0$, $1.0 < z < 1.5$, and $1.5 < z < 2.5$, respectively, following Whitaker et al. (2010) and Brammer et al. (2009), the fraction of quiescent galaxies in the red sequence population is 46% (55% in the red sequence galaxies with $M_{\text{star}} > 10^{11} M_{\odot}$), 36% (40%), and 32% (32%) for the redshift bins. Since most quiescent galaxies show the rest $U - V \sim 1.2$ or bluer, we adopt $U - V = 1.2$ (horizontal dashed line in the figure) as a reference to determine the limiting stellar mass for the galaxies in the wide and deep fields. At $1.5 < z < 2.5$, we can nearly completely sample the galaxies down to $\sim 10^{10.5} M_{\odot}$ for the wide field and to $\sim 10^{10} M_{\odot}$ for the deep field. In the following, we use quiescent galaxies with $M_{\text{star}} > 10^{10.5} M_{\odot}$ in the wide field and those with $M_{\text{star}} > 10^{10} M_{\odot}$ in the deep field as a mass-limited quiescent sample at $1.5 < z < 2.5$. For the $0.5 < z < 1.0$ and $1.0 < z < 1.5$ redshift bins, we also limit the quiescent sample to those with $M_{\text{star}} > 10^{10} M_{\odot}$ for a fair comparison with the $1.5 < z < 2.5$ bin, while the limiting stellar mass is lower than $10^{10} M_{\odot}$ in the both fields for these redshift bins. The number of galaxies in the mass-limited quiescent sample is 130 at $0.5 < z < 1.0$, 70 at $1.0 < z < 1.5$ and 50 at $1.5 < z < 2.5$.

It should be noted that our multi-band data other than K_s -band are also deep enough to select quiescent galaxies down to the limiting stellar mass mentioned above. For example, even quiescent objects at $z \sim 2$ – 2.5 with $M_{\text{star}} > 10^{10} M_{\odot}$ ($> 10^{10.5} M_{\odot}$ for the wide field) whose stellar age is as old as the age of the universe are expected to be detected at least in H , $3.6\mu\text{m}$, and $4.5\mu\text{m}$ bands at $S/N > 2$ in addition to the K_s -band detection (also in J band for $z \lesssim 2.3$). Furthermore, deep HST/ACS data are deep enough to detect at least quiescent objects with $M_{\text{star}} = 10^{10} M_{\odot}$ and with stellar age of ~ 0.6 – 1.0 Gyr in V , i , and z bands at $z < 2.5$. Therefore we can judge whether the criteria for the quiescent population are satisfied or not for galaxies with $M_{\text{star}} \sim 10^{10} M_{\odot}$ even at $z \sim 2$ – 2.5 . For dusty

galaxies, however, it could not be the case. Objects with large extinction are often not detected in the ACS images, and the uncertainty in age/τ of these objects tend to be large. In fact, galaxies with large errorbars in the upper panels of Figure 1 have relatively red SEDs in the NIR–MIR region and are fitted with dusty model templates. Since the number of such objects in the quiescent sample is small, however, the contamination from heavily obscured star-forming galaxies does not seem to affect our results in the following.

Figure 2 shows the uncertainty of the estimated stellar mass for the quiescent galaxies. At $M_{\text{star}} \gtrsim 10^{10} M_{\odot}$, the stellar mass errors are relatively small and typically < 0.2 dex. Furthermore, as seen in the next section, the low-mass slope of the stellar mass function for quiescent galaxies are nearly flat or slightly positive ($\alpha \sim 0$ – 0.6). Since it suggests that the number density of low-mass quiescent galaxies is relatively small, the contamination from lower-mass galaxies could not be significant even if these low-mass galaxies have slightly larger stellar mass errors. Therefore the incompleteness and contamination due to the stellar mass error are expected to be negligible.

5. Results

The left panel of Figure 3 shows the stellar mass function (hereafter, SMF) of quiescent galaxies selected in the previous section in the different redshift bins. For comparison, those for star-forming galaxies with $\text{age}/\tau < 4$ and all stellar mass-selected galaxies are also shown. We use the V_{max} method to calculate the comoving number density. K09 calculated the V_{max} for the K_s -band magnitude limit ($K_s = 23$ for the wide field or $K_s = 24$ for the deep field) by using the best-fit model template for each object (see Section 3.3 in K09 for details).

It is seen that the number density of quiescent galaxies gradually increases from $1.5 < z < 2.5$ to $0.5 < z < 1.0$ in all mass ranges. The increase of the number density seems to be nearly independent of stellar mass over 10^{10} –

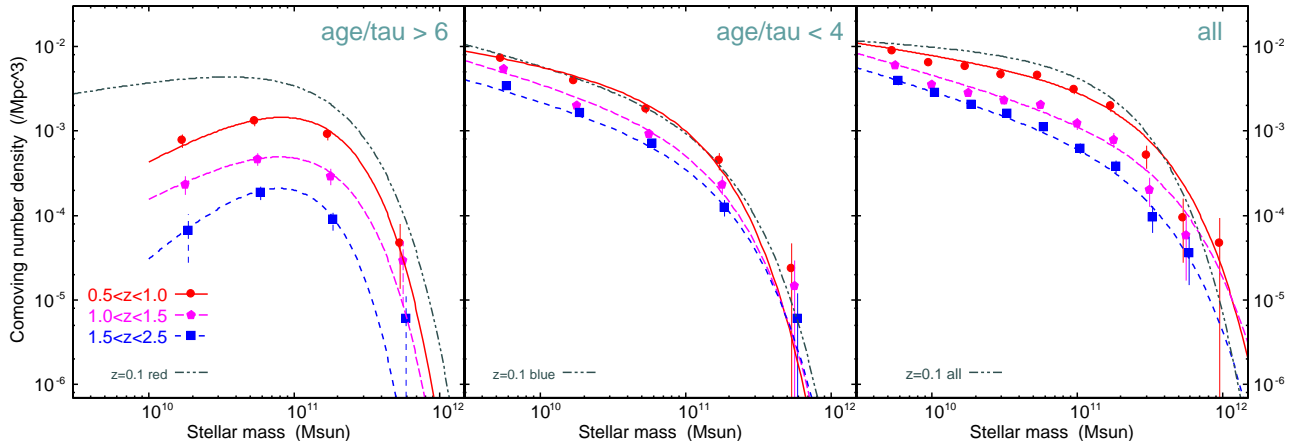


Fig. 3. The evolution of the stellar mass function of quiescent galaxies with $\text{age}/\tau > 6$ (left), star-forming galaxies with $\text{age}/\tau < 4$ (middle), and all stellar mass-selected galaxies (right, from K09). Circles, pentagons, and squares show the results calculated with the $1/V_{\text{max}}$ formalism for galaxies at $0.5 < z < 1.0$, $1.0 < z < 1.5$, and $1.5 < z < 2.5$, respectively. Error bars are based on the Poisson statistics. Solid, long-dashed, and short-dashed lines represent the results with the STY method for galaxies at $0.5 < z < 1.0$, $1.0 < z < 1.5$, and $1.5 < z < 2.5$, respectively. For reference, the local SMF for all, red, and blue galaxies at $z \sim 0.1$ by Bell et al. (2003) is shown as the double-dotted dashed line in each panel.

$10^{11.5} M_{\odot}$. The number density increases by a factor of ~ 3 from $1.0 < z < 1.5$ to $0.5 < z < 1.0$ and by a factor of ~ 10 from $1.5 < z < 2.5$ to $0.5 < z < 1.0$ in this mass range. On the other hand, the number density of star-forming galaxies with $\text{age}/\tau < 4$ increases only by a factor of ~ 1.9 from $1.0 < z < 1.5$ to $0.5 < z < 1.0$ and by a factor of ~ 2.8 from $1.5 < z < 2.5$ to $0.5 < z < 1.0$. The number density evolution of quiescent galaxies is clearly stronger than that of star-forming galaxies.

In order to evaluate the shape of the SMF, we used the STY method (Sandage et al. 1979) assuming the Schechter function form (Schechter 1976) as in K09. We estimated the best-fit values of the Schechter parameters, namely, the characteristic mass M^* and the low-mass slope α for both the quiescent sample and the star-forming galaxies. For the star-forming galaxies, we used the same limiting stellar mass as a function of redshift as in K09, which is estimated by using the 90 percentile of $U - V$ color at each stellar mass for all stellar mass-selected galaxies (see Section 3.2 of K09 for details). Such limiting stellar mass is probably suitable (or conservative) for the star-forming galaxies, because these galaxies tend to have relatively low stellar M/L ratios except for extremely dusty galaxies. Further details of estimating the Schechter parameters with the STY method are explained in Section 3.3 of K09.

Figure 4 shows the best-fit Schechter parameters and their uncertainty in the $M^* - \alpha$ plane for each redshift bin. The best-fit values and their uncertainty are also summarized in Table 1. For comparison, we also show the best-fit M^* and α for all stellar mass-selected galaxies estimated by K09. The low-mass slope α for the quiescent sample is significantly flatter than those for the star-forming and all stellar mass-selected samples over $0.5 < z < 2.5$, although the uncertainty of α for these quiescent galaxies is relatively large due to the small number of the sample and the relatively high limiting stellar mass. On the

other hand, the characteristic mass M^* for the quiescent sample is similar with that for the star-forming galaxies, while it could be slightly smaller than the star-forming galaxies at $1.5 < z < 2.5$. The M^* for the both quiescent and star-forming samples is lower than that for all mass-selected galaxies by a factor of ~ 2 . This may be due to the effects of the combination of the (quiescent and star-forming) mass functions with different shapes (different α). K09 found a marginal upturn around $\sim 10^{10} M_{\odot}$ in the stellar mass function for the stellar mass-selected sample, which cannot be fitted very well with the single Schechter function form. On the other hand, the SMF for the star-forming galaxies seems to have a very weak or no upturn, and is fitted with the Schechter function better than that for all mass-selected galaxies in all redshift bins. The contribution of the flatter mass function of quiescent galaxies at $M_{\text{star}} \gtrsim 10^{10} M_{\odot}$ could cause the upturn in the SMF for all mass-selected galaxies, which has been observed at $z < 1$ (e.g., Drory et al. 2009; Peng et al. 2010). Fitting the mass function with such a upturn with the single Schechter function may lead to the slightly higher M^* .

We found no significant evolution of the shape of the SMF for the quiescent sample. Although M^* and α for these galaxies might become slightly lower and more positive values respectively at $1.5 < z < 2.5$, the large uncertainty prevents us from confirming this. The evolution of the shape of the SMF for the star-forming galaxies is similar with that for all mass-selected galaxies; the low-mass slope becomes slightly steeper with redshift at $z > 1$, while the characteristic mass does not evolve significantly.

Figure 5 shows the fraction of quiescent galaxies at each stellar mass for the different redshift bins. The fraction of quiescent galaxies increases with stellar mass over $10^{10} - 10^{11.5} M_{\odot}$ in all redshift bins, though the uncertainty of the fraction at $> 10^{11.5} M_{\odot}$ is very large due to the very small number of such massive quiescent galaxies in our

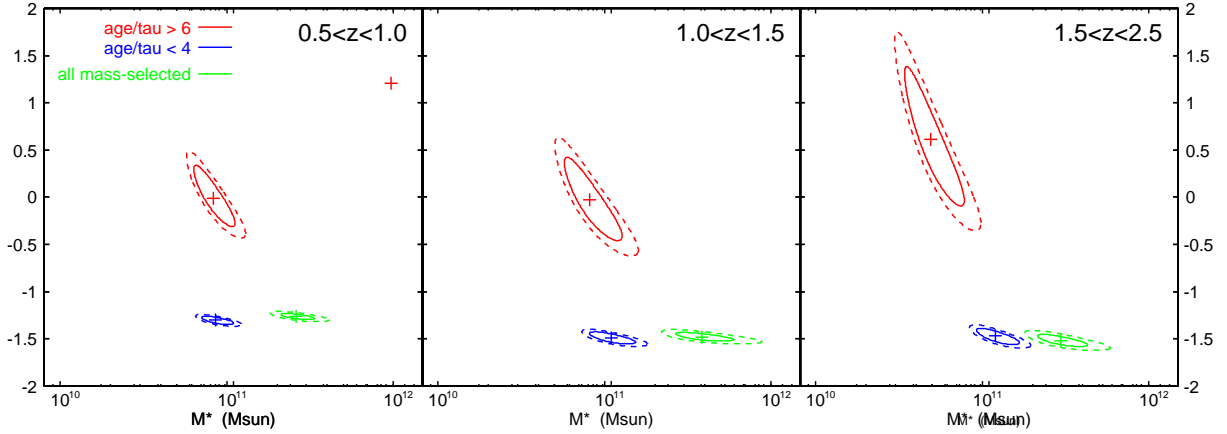


Fig. 4. The Schechter parameters in M^* – α plane for the quiescent (red), star-forming (blue), and all stellar mass-selected (green) samples in each redshift bin. Crosses show the best-fit values determined with the STY method. 1σ (solid) and 2σ (dashed) error contours are also shown.

Table 1. Best-fit M^* and α obtained with the STY method for quiescent and star-forming galaxies

redshift	quiescent (age/ $\tau > 6$)		star-forming (age/ $\tau < 4$)		all mass-selected (from K09)	
	$\log_{10} M^* (M_{\odot})$	α	$\log_{10} M^* (M_{\odot})$	α	$\log_{10} M^* (M_{\odot})$	α
$0.5 < z < 1.0$	$10.92^{+0.08}_{-0.08}$	$-0.01^{+0.23}_{-0.19}$	$10.93^{+0.07}_{-0.05}$	$-1.30^{+0.02}_{-0.03}$	$11.33^{+0.10}_{-0.07}$	$-1.26^{+0.03}_{-0.03}$
$1.0 < z < 1.5$	$10.91^{+0.12}_{-0.10}$	$-0.03^{+0.29}_{-0.29}$	$11.04^{+0.09}_{-0.09}$	$-1.49^{+0.04}_{-0.04}$	$11.48^{+0.16}_{-0.13}$	$-1.48^{+0.04}_{-0.04}$
$1.5 < z < 2.5$	$10.69^{+0.12}_{-0.10}$	$+0.61^{+0.49}_{-0.47}$	$11.08^{+0.09}_{-0.07}$	$-1.47^{+0.05}_{-0.06}$	$11.38^{+0.14}_{-0.12}$	$-1.52^{+0.06}_{-0.06}$

sample (1–2 such galaxies in each bin). This mass dependence of the fraction of quiescent galaxies over $0.5 < z < 2.5$ is consistent with the above result that the shape of the SMF for these galaxies is flatter than those for the star-forming galaxies. On the other hand, the fraction of quiescent galaxies at each mass decreases with redshift (increases with time) over 10^{10} – $10^{11.5} M_{\odot}$. The quiescent fraction of galaxies with $M_{\text{star}} = 10^{11}$ – $10^{11.5} M_{\odot}$ increases from $\sim 25\%$ at $1.5 < z < 2.5$ to $\sim 50\%$ at $0.5 < z < 1.0$, while that of galaxies with $M_{\text{star}} = 10^{10}$ – $10^{10.5} M_{\odot}$ increases from $\lesssim 5\%$ to $\sim 15\%$ in the same redshift range. This is also consistent with the stronger evolution in the number density of quiescent galaxies than that of the star-forming galaxies mentioned above.

6. Discussion

6.1. Comparison with other studies

We have investigated the evolution of the number density and the fraction of quiescent galaxies as a function of stellar mass at $0.5 < z < 2.5$, using the very deep NIR data of the MODS and the multi-wavelength ancillary data of the GOODS. Here we compare our results with previous studies in other general fields.

Vergani et al. (2008) investigated the evolution of early-type galaxies selected by spectral classification with the D_n4000 index up to $z \sim 1.3$, using the VVDS spectroscopic sample ($I_{\text{AB}} < 24$). They found that the low-mass slope of the SMF for early-type galaxies is flatter ($\Delta\alpha \sim 1$) than those of star-forming and overall galaxy population. The

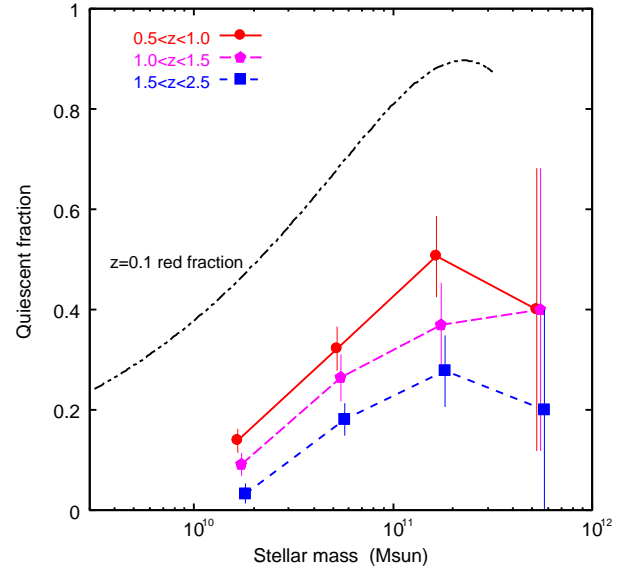


Fig. 5. Fraction of quiescent galaxies as a function of stellar mass. Circles, pentagons, and squares represent galaxies at $0.5 < z < 1.0$, $1.0 < z < 1.5$, and $1.5 < z < 2.5$, respectively. Error bars are based on the Poisson statistics. For reference, the red fraction for galaxies at $z \sim 0.1$ from Bell et al. (2003) is shown as the double-dotted dashed line.

number density of early-type galaxies increases by a factor of ~ 3 between $1.0 < z < 1.3$ and $0.7 < z < 1.0$, while that of late-type galaxies increases by a factor of ~ 2 in the same redshift range. Our results seen in the $0.5 < z < 1.0$ and $1.0 < z < 1.5$ bins are consistent with these results of

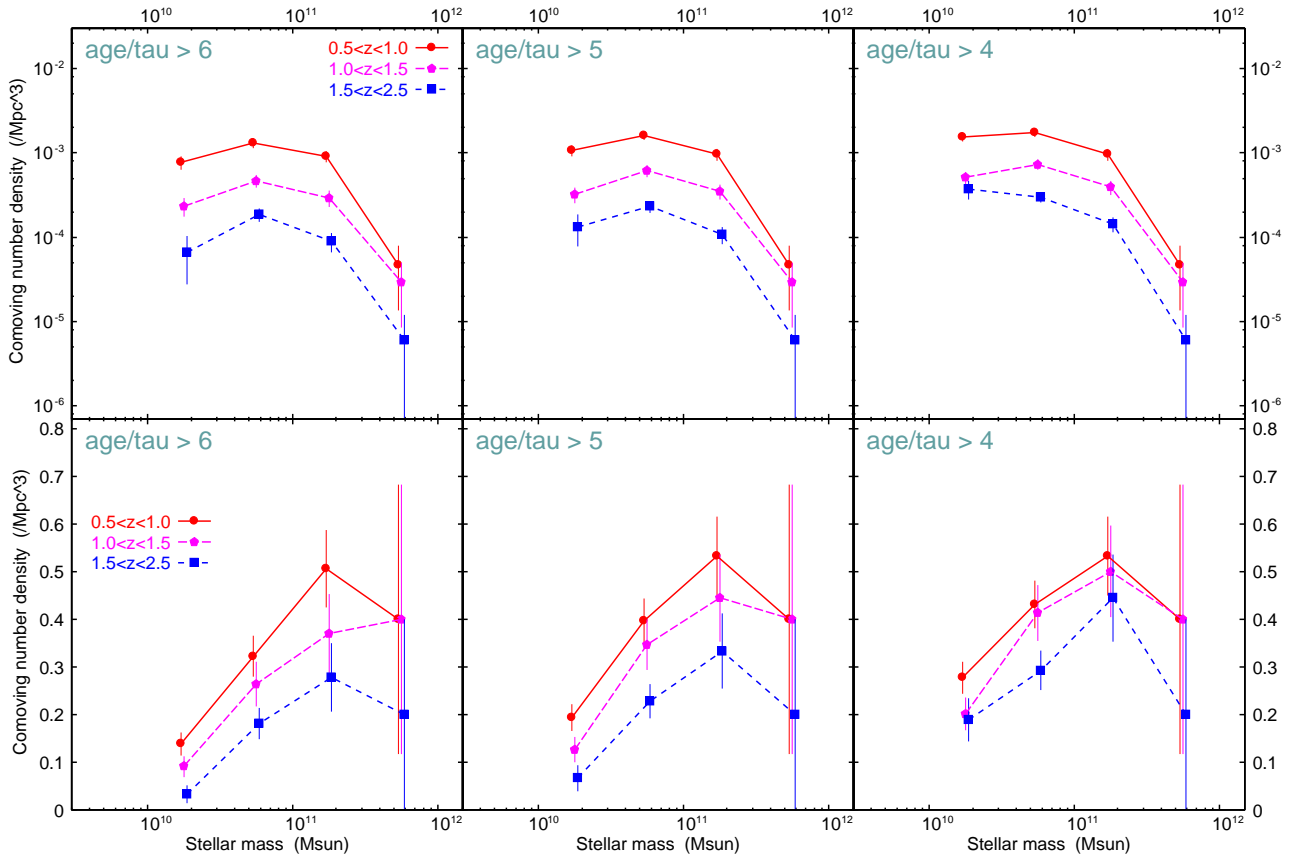


Fig. 6. Number density and fraction of quiescent galaxies as a function of stellar mass for the different criteria of $\text{age}/\tau > 6$ (left), $\text{age}/\tau > 5$ (middle), and $\text{age}/\tau > 4$ (right). Symbols are the same as Figure 5.

Vergani et al. (2008).

Ilbert et al. (2010) also studied the evolution of the SMF of quiescent galaxies selected by a color selection with the rest-frame $NUV - r'$ and $r' - J$ up to $z \sim 2$, using the Spitzer/IRAC $3.6\mu\text{m}$ -selected sample ($m_{\text{AB}} < 23.9$) in the COSMOS 2 deg^2 field. Although their sample reach only to $\sim 10^{11} M_{\odot}$ at $z \gtrsim 1.5$, they estimated the low-mass slope of the SMF for quiescent galaxies up to $z \sim 1.2$, and found that the low-mass slope for these galaxies gradually flatten with redshift and becomes $\alpha \sim 0$ at $z \sim 0.8$. The number density of these quiescent galaxies increases by a factor of ~ 3 from $z \sim 1.2$ to $z \sim 0.7$ and by a factor of ~ 10 from $z \sim 2$ to $z \sim 0.7$. Such evolution of quiescent galaxies is consistent with our results seen in the previous section. We found that the flat low-mass slope for these galaxies continues up to $z \sim 2$. Ilbert et al. (2010) also pointed out that the evolution of the SMF for star-forming galaxies over $0.2 < z < 2$ is relatively weak and that the number density of star-forming galaxies increases by a factor of ~ 2.5 between $z \sim 2$ and $z \sim 0.9$. The star-forming galaxies with $\text{age}/\tau < 4$ in our sample also show the similar evolution (the middle panel of Figure 3).

Fontana et al. (2009) investigated the evolution of the fraction of “red and dead” galaxies with $\text{age}/\tau > 6$ among massive galaxies with $M_{\text{star}} > 7 \times 10^{10} M_{\odot}$ up to $z \sim 3.5$, using the GOODS-MUSIC sample in the GOODS-South field. Since the survey field layout, the filter set used in

the SED fitting, and the sample selection in this study are similar with those in Fontana et al. (2009), a direct comparison is possible. They found that the fraction of the “red and dead” galaxies gradually decreases with redshift, and Figure 5 in Fontana et al. (2009) shows that the fraction is $\sim 50\%$ at $z \sim 0.7$, $\sim 40\%$ at $z \sim 1.2$, and $\sim 20\%$ at $z \sim 2$. If we limit our quiescent sample to those with $M_{\text{star}} > 7 \times 10^{10} M_{\odot}$ as in Fontana et al. (2009), the fraction of quiescent galaxies becomes 52% at $0.5 < z < 1.0$, 37% at $1.0 < z < 1.5$, and 29% at $1.5 < z < 2.5$. We estimated the cosmic variance for these galaxies with the method introduced by Moster et al. (2010), using the clustering strength of $r_0 \sim 10 \text{ Mpc}$ for quiescent galaxies at $1 \lesssim z \lesssim 2$ observed by Williams et al. (2009) and Hartley et al. (2010). The correlation length of $r_0 \sim 10 \text{ Mpc}$ corresponds to the galaxy bias of $b_g \sim 2$ at $z \sim 0.75$, $b_g \sim 3$ at $z \sim 1.25$, and $b_g \sim 4.5$ at $z \sim 2$. The resulting relative cosmic variance for our quiescent sample is $\sigma_v \sim 0.24$ at $0.5 < z < 1.0$, $\sigma_v \sim 0.30$ at $1.0 < z < 1.5$, and $\sigma_v \sim 0.26$ at $1.5 < z < 2.5$. If we take account of the cosmic variance and Poisson errors, the quiescent fractions in this study and Fontana et al. (2009) agree well within the uncertainty.

On the other hand, Grazian et al. (2007) presented the SMF for galaxies with $\text{age}/\tau > 4$ and those with $\text{age}/\tau < 4$ at $1.4 < z < 2.5$. In order to compare our results directly with those in Grazian et al. (2007) and to check the effect of changing the selection criterion to our re-

sults, we estimated the SMF and the fraction of galaxies with $\text{age}/\tau > 4$ and 5 as a function of stellar mass, and compared them with those of galaxies with $\text{age}/\tau > 6$ in Figure 6. Although the overall trend does not change significantly when the criteria of $\text{age}/\tau > 5$ and 4 are used, the low-mass slope becomes slightly steeper and the evolution of the number density becomes weaker as the selection threshold is loosened. This may be due to the gradual increase of the contamination from galaxies with star formation activities. For example, the fraction of massive quiescent galaxies with $M_{\text{star}} = 10^{11}\text{--}10^{11.5} M_{\odot}$ already reaches to $\sim 50\%$ at $z \sim 2$ in the case with $\text{age}/\tau > 4$. This is consistent with the similar number densities of galaxies with $\text{age}/\tau > 4$ and $\text{age}/\tau < 4$ at $M_{\text{star}} \sim 10^{11} M_{\odot}$ seen in Figure 8 of Grazian et al. (2007).

In summary, the shape of the SMF of quiescent galaxies at $z \sim 1$ and the number density evolution of massive quiescent galaxies with $M_{\text{star}} \gtrsim 10^{11} M_{\odot}$ at $1 \lesssim z \lesssim 2$ seen in the previous section are consistent with the previous studies in other general fields. Thus, the field-to-field variance does not seem to significantly affect our results. Furthermore, in this paper, we found that the evolution of the number density of quiescent galaxies with relatively low stellar mass ($\sim 10^{10}\text{--}10^{11} M_{\odot}$) is similar with that of massive ones, and that the flat low-mass slope of quiescent galaxies continues up to $z \sim 2$.

6.2. Quenching of star formation and mass-dependent evolution of galaxies

In Section 5, we found that the number density of quiescent galaxies with $\text{age}/\tau > 6$ increases by a factor of ~ 3 from $1.0 < z < 1.5$ to $0.5 < z < 1.0$ and by a factor of ~ 10 from $1.5 < z < 2.5$ to $0.5 < z < 1.0$ over $M_{\text{star}} = 10^{10}\text{--}10^{11.5} M_{\odot}$. We note that the number density of galaxies at $0.5 < z < 1.0$ in our sample could be slightly overestimated due to the known large-scale structures around the HDF-North (K09; Wirth et al. 2004). Nevertheless, the rapid increase of the number of quiescent galaxies in the universe seems to occur at $1 \lesssim z \lesssim 2$. Furthermore, the evolution of the number density is nearly independent of stellar mass. The low-mass slope of the SMF for these quiescent galaxies is significantly flatter than those for star-forming and all stellar mass-selected galaxies over $0.5 < z < 2.5$. The fraction of quiescent galaxies for massive galaxies is higher than that for low-mass galaxies in the redshift range. Here we consider that the increase of quiescent galaxies is caused by the cessation of star formation in some fraction of star-forming galaxies as in previous studies at $z < 1$ (e.g., Bell et al. 2007; Peng et al. 2010). Since the number density of quiescent galaxies rapidly increases by a factor of ~ 3 between $z \sim 2$ and $z \sim 1.25$ (~ 1.6 Gyr) and by a factor of ~ 3 between $z \sim 1.25$ and $z \sim 0.75$ (~ 2.3 Gyr), the quenching of star formation is expected to occur preferentially in more massive galaxies over $1 \lesssim z \lesssim 2$ in order to maintain the mass-dependence of the fraction of quiescent galaxies mentioned above. We estimated the quenching rate as a function of stellar mass by calculating the fraction of newly emerging quiescent galaxies between the redshift bins relative to the

star-forming population including newly increased galaxies at a given stellar mass range. For simplicity, other processes affecting this fraction such as the hierarchical merging is ignored. As a result, we expect that 7%, 18% and 29% of the star-forming galaxies with $M_{\text{star}} = 10^{10}\text{--}10^{10.5} M_{\odot}$, $10^{10.5}\text{--}10^{11} M_{\odot}$ and $10^{11}\text{--}10^{11.5} M_{\odot}$ ceased star formation between $1.5 < z < 2.5$ and $1.0 < z < 1.5$, respectively, and 10%, 23% and 41% of the star-forming galaxies with the same stellar mass ranges became quiescent between $1.0 < z < 1.5$ and $0.5 < z < 1.0$. It seems that more massive star-forming galaxies tend to cease star formation preferentially at $1 \lesssim z \lesssim 2$. Recently, Peng et al. (2010) reported that such a mass-dependent quenching process could explain no evolution of the shape of the SMF for star-forming galaxies and the flatter low-mass slope and the similar characteristic mass for passive galaxies at $z < 1$. Such ‘‘mass quenching’’ might work even at $1 \lesssim z \lesssim 2$, when the rapid increase of the number density of quiescent galaxies was observed. The characteristic mass M^* of the SMF for the star-forming galaxies with $\text{age}/\tau < 4$ in our sample shows no significant evolution at the redshift range (middle panel of Figure 3), which seems to be also consistent with the prediction by Peng et al. (2010).

K09 found the mass-dependent evolution of the number density for all stellar mass-selected galaxies at $z \gtrsim 1\text{--}1.5$. The number density of galaxies with $M_{\text{star}} \sim 10^{11} M_{\odot}$ more strongly evolves than that for galaxies with $M_{\text{star}} \sim 10^{10} M_{\odot}$ (right panel of Figure 3). On the other hand, the increase of the number density of quiescent galaxies is nearly independent of stellar mass as discussed above. The mass dependence of the evolution for star-forming galaxies is also rather weak (middle panel of Figure 3). The mass-dependent evolution for all population could be explained by the differences between the quiescent and star-forming populations in the strength of the evolution of the number density and in the shape of the SMF. The quiescent population has the flatter low-mass slope of the SMF and shows the stronger evolution of the number density than star-forming galaxies. Therefore the rapid increase of quiescent galaxies contributes strongly to the number density evolution for galaxies with $\sim 10^{11} M_{\odot}$, while their contribution is negligible for those with $\sim 10^{10} M_{\odot}$ because of the rather low fraction of these galaxies. In this context, the more rapid increase of the number density of $\sim M^*$ galaxies than lower-mass galaxies at $z \gtrsim 1\text{--}1.5$ found in K09 might be explained by a mass-dependent quenching mechanism which preferentially ceases star formation in these massive galaxies.

In Yamada et al. (2009), we found that X-ray selected AGNs at $2 < z < 4$ are preferentially associated with more massive galaxies, and that $\sim 30\%$ of galaxies with $M_{\text{star}} > 10^{11} M_{\odot}$ show the AGN activity with the X-ray luminosity larger than $\sim 10^{42} \text{ erg s}^{-1}$. Brusa et al. (2009) also found a similar mass-dependence of the AGN fraction at $1 \lesssim z \lesssim 4$. The AGN feedback may be related with the mass-dependent star formation quenching. Bundy et al. (2008) investigated the fractions of red galaxies and X-ray selected AGNs in stellar mass-selected galaxies at

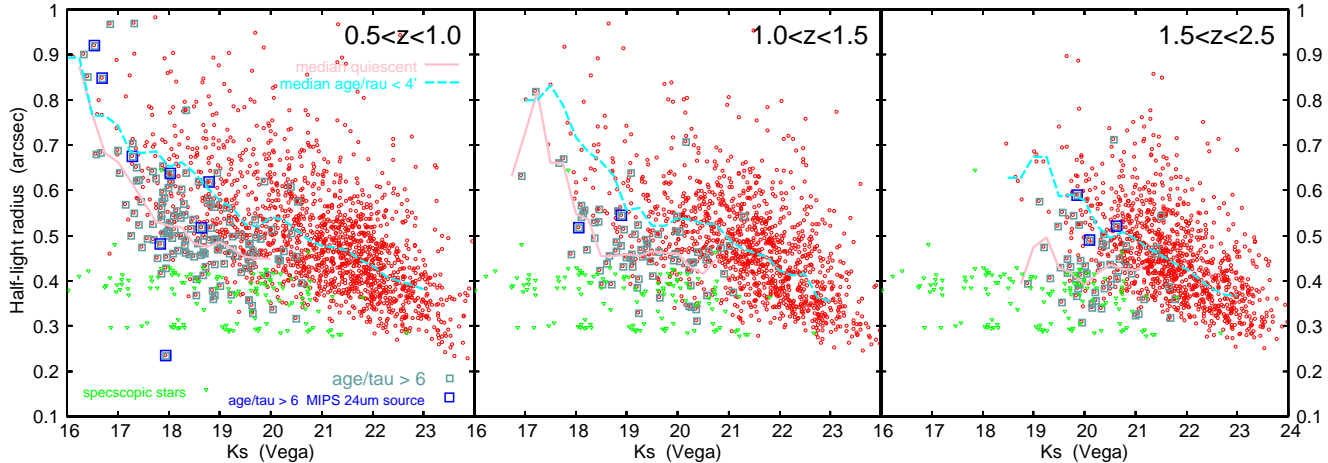


Fig. 7. Half light radius in the observed K_s band vs. K_s -band magnitude for K_s -selected galaxies in each redshift bin. Gray squares represent the mass-selected ($M_{\text{star}} > 10^{10} M_{\odot}$) quiescent galaxies with $\text{age}/\tau > 6$. Larger blue squares show MIPS $24\mu\text{m}$ sources with $\text{age}/\tau > 6$. Solid and dashed lines represent the median values for the quiescent sample and star-forming galaxies with $\text{age}/\tau < 4$ at each magnitude, respectively. It should be noted that the K_s -band half light radii are measured on the mosaic image where the PSF varies among the different pointings of MOIRCS (FWHM = 0.45–0.60 arcsec, see Kajisawa et al. 2011 for details). For reference, spectroscopically confirmed stars are shown as green triangles in each panel.

$0.4 < z < 1.4$ as a function of stellar mass to compare the star formation quenching rate with the AGN triggering rate. They found that the mass-dependence and normalization of the both rates agree well, although the estimated normalization of the AGN triggering rate depends strongly on the assumed AGN lifetime. In order to compare our results with the star formation quenching rate in Bundy et al. (2008), we divided the quenching rates calculated above by the time intervals between the redshift bins. The results are 4% Gyr^{-1} , 10% Gyr^{-1} , and 18% Gyr^{-1} between $z \sim 1.25$ and $z \sim 0.75$ for galaxies with 10^{10} – $10^{10.5} M_{\odot}$, $10^{10.5}$ – $10^{11} M_{\odot}$, and 10^{11} – $10^{11.5} M_{\odot}$, respectively, and 4% Gyr^{-1} , 11% Gyr^{-1} , and 18% Gyr^{-1} between $z \sim 2$ and $z \sim 1.25$ for the same mass ranges. Both the mass-dependence and normalization are consistent with the results of Bundy et al. (2008), although the selection of quiescent galaxies is different between Bundy et al. (2008) (rest-frame $U - B$ color) and this study (age/τ from the SED fitting). Our results may also suggest that the star formation quenching rate per unit time at a given stellar mass seems to be roughly constant over $1 \lesssim z \lesssim 2$. In a future work, we will study the evolution of the AGN hosts in the MODS field at $1 \lesssim z \lesssim 2$ and compare it with the star formation quenching rate estimated here.

On the other hand, several studies reported that the clustering of quiescent galaxies is stronger than that of star-forming galaxies even at $z \sim 2$ (Hartley et al. 2008; Hartley et al. 2010; Williams et al. 2009), which implies that quiescent galaxies tend to inhabit more massive dark matter halos when their number density rapidly increases. Therefore the dark matter halo mass may play some role in the quenching of star formation. Williams et al. (2009) and Hartley et al. (2010) pointed out the possibility that the clustering strength of quiescent galaxies at $1 \lesssim z \lesssim 2$ is nearly independent of their rest-frame K -band luminosity

(approximately stellar mass), while it is observed at the same redshift range that the clustering strength of the overall galaxy population is correlated with stellar mass (e.g., Ichikawa et al. 2007; Foucaud et al. 2010; Wake et al. 2010). There may be a critical halo mass above which gas cooling and star formation are shut down, for example, due to the shock heating (e.g., Dekel & Birnboim 2006; Cattaneo et al. 2006). In this scenario, the (stellar) mass-dependent quenching of star formation could be explained if massive star-forming galaxies tend to inhabit more massive dark matter halos than low-mass star-forming ones, which is naturally predicted by theoretical models where the star formation activity is simply regulated by the gas (and dark matter) accretion rate in the halo (e.g., Bouché et al. 2010). In this context, it is interesting to investigate the mass-dependence of the clustering strength for quiescent and star-forming samples at $1 \lesssim z \lesssim 2$ more intensively.

The quenching of star formation may be also related with the surface stellar mass density of galaxies. Several studies at low and high redshifts reported that the rest-frame color or specific star formation rate of galaxies are strongly correlated with their surface stellar mass density (e.g., Kauffmann et al. 2006; Franx et al. 2008; Williams et al. 2010). Most galaxies with the surface mass density higher than a threshold value have red color and low star formation activities at each redshift. The threshold surface density seems to increase with redshift gradually. At $z \sim 2$, many studies have found massive quiescent galaxies with much smaller sizes (e.g., $R_e \sim 1$ kpc) than the present massive ellipticals (Daddi et al. 2005; Zirm et al. 2007; Longhetti et al. 2007; Cimatti et al. 2008; van Dokkum et al. 2008; Damjanov et al. 2009; Ryan et al. 2010). Quiescent galaxies in our sample also tend to have small half light radii in the observed K_s band relative to star-forming galaxies with similar K_s -band magnitudes

(Figure 7). Considering their higher stellar M/L ratio and smaller size than star-forming galaxies, these quiescent galaxies are expected to have higher surface stellar mass densities. At $1.5 < z < 2.5$, there are also K_s -bright quiescent galaxies whose sizes cannot be distinguished from point sources. Since compact galaxies with $R_e \sim 1$ kpc at $z \gtrsim 1$ are expected not to be resolved in the MODS K_s -band image, these galaxies may be such compact quiescent objects. In order to estimate the surface stellar mass density of galaxies quantitatively and investigate the relation between the mass-dependent evolution of quiescent galaxies and the surface stellar mass density, we need a detailed analysis of the surface brightness profiles which takes account of the seeing effect or higher-resolution NIR data such as those with *HST*/WFC3.

7. Summary

We have investigated the evolution of quiescent galaxies at $0.5 < z < 2.5$ in the GOODS-North field as a function of stellar mass, using the very deep NIR data of the MODS and the public multi-wavelength data of the GOODS. We performed the SED fitting of the multi broad-band photometry with the GALAXEV population synthesis model and selected galaxies with $\text{age}/\tau > 6$ and without the MIPS $24\mu\text{m}$ detection ($f_{24\mu\text{m}} \lesssim 20\mu\text{Jy}$) as the quiescent population. The deep MODS data allow us to construct a stellar mass-limited sample of quiescent galaxies down to $\sim 10^{10} M_\odot$ even at $z \sim 2$ for the first time. Main results in this study are as follows.

- The number density of quiescent galaxies rapidly increases by a factor of ~ 3 from $1.0 < z < 1.5$ to $0.5 < z < 1.0$ and by a factor of ~ 10 from $1.5 < z < 2.5$ to $0.5 < z < 1.0$. On the other hand, that of star-forming galaxies with $\text{age}/\tau < 4$ increases only by factors of ~ 2 and ~ 3 in the same redshift ranges.
- The increase of the number density of quiescent galaxies is nearly independent of stellar mass over 10^{10} – $10^{11.5} M_\odot$, and these galaxies show no significant evolution in the shape of the SMF.
- The low-mass slope of the SMF for these quiescent galaxies is $\alpha \sim 0$ – 0.6 , which is significantly flatter than those of the star-forming galaxies and all stellar mass-selected galaxies ($\alpha \sim -1.3$ – -1.5).
- The fraction of quiescent galaxies increases with stellar mass over $0.5 < z < 2.5$, and decreases with redshift over 10^{10} – $10^{11.5} M_\odot$; the quiescent fraction of galaxies with 10^{11} – $10^{11.5} M_\odot$ increases from $\sim 25\%$ at $1.5 < z < 2.5$ to $\sim 50\%$ at $0.5 < z < 1.0$, while that of galaxies with 10^{10} – $10^{10.5} M_\odot$ increases from $\lesssim 5\%$ to $\sim 15\%$ in the same redshift range.
- Provided that the increase of the number density of quiescent galaxies is caused by the quenching of star formation in some star-forming galaxies, the quenching process is expected to be more effective in more massive galaxies in order to maintain the mass-dependence of the fraction of quiescent galaxies over $0.5 < z < 2.5$.

- Since the mass dependence of the evolution of the number density of star-forming galaxies is also weak, stronger evolution of quiescent galaxies with the flatter shape of the SMF would cause the more rapid increase of the number density of galaxies with $M_{\text{star}} \sim 10^{11} M_\odot$ than lower-mass galaxies at $1 \lesssim z \lesssim 2$.

We thank an anonymous referee for very helpful suggestions and comments. We also thank Yoshi Taniguchi for useful discussions. This study is based on data collected at Subaru Telescope, which is operated by the National Astronomical Observatory of Japan. This work is based in part on observations made with the Spitzer Space Telescope, which is operated by the Jet Propulsion Laboratory, California Institute of Technology under a contract with NASA. Some of the data presented in this paper were obtained from the Multi-mission Archive at the Space Telescope Science Institute (MAST). STScI is operated by the Association of Universities for Research in Astronomy, Inc., under NASA contract NAS5-26555. Support for MAST for non-HST data is provided by the NASA Office of Space Science via grant NAG5-7584 and by other grants and contracts. Data reduction and analysis were carried out on common use data analysis computer system at the Astronomy Data Center, ADC, of the National Astronomical Observatory of Japan. IRAF is distributed by the National Optical Astronomy Observatories, which are operated by the Association of Universities for Research in Astronomy, Inc., under cooperative agreement with the National Science Foundation.

References

- Abraham, R. G., et al. 2007, *ApJ*, 669, 184
 Alexander, D. M., et al. 2003, *AJ*, 126, 539
 Arnouts, S., et al. 2007, *A&A*, 476, 137
 Baldry, I. K., Glazebrook, K., Brinkmann, J., Ivezić, Ž., Lupton, R. H., Nichol, R. C., & Szalay, A. S. 2004, *ApJ*, 600, 681
 Barger, A. J., Cowie, L. L., & Wang, W.-H. 2008, *ApJ*, 689, 687
 Bell, E. F., McIntosh, D. H., Katz, N., & Weinberg, M. D. 2003, *ApJS*, 149, 289
 Bell, E. F., et al. 2004, *ApJ*, 608, 752
 Bell, E. F., Zheng, X. Z., Papovich, C., Borch, A., Wolf, C., & Meisenheimer, K. 2007, *ApJ*, 663, 834
 Bertin E., Arnouts S., 1996, *A&AS*, 117, 393
 Borch, A., et al. 2006, *A&A*, 453, 869
 Bouché, N., et al. 2010, *ApJ*, 718, 1001
 Brammer, G. B., et al. 2009, *ApJL*, 706, L173
 Brinchmann, J., & Ellis, R. S. 2000, *ApJL*, 536, L77
 Brinchmann, J., Charlot, S., White, S. D. M., Tremonti, C., Kauffmann, G., Heckman, T., & Brinkmann, J. 2004, *MNRAS*, 351, 1151
 Brusa, M., et al. 2009, *A&A*, 507, 1277
 Bruzual G., Charlot S., 2003, *MNRAS*, 344, 1000
 Bundy, K., et al. 2006, *ApJ*, 651, 120
 Bundy, K., et al. 2008, *ApJ*, 681, 931
 Calzetti, D., Armus, L., Bohlin, R. C., Kinney, A. L., Koornneef, J.,

- Cameron, E., Carollo, C. M., Oesch, P. A., Bouwens, R. J., Illingworth, G. D., Trenti, M., Labbe, I., & Magee, D. 2010, arXiv:1007.2422
- Capak, P., et al. 2004, *AJ*, 127, 180
- Cassata, P., et al. 2008, *A&A*, 483, L39
- Cattaneo, A., Dekel, A., Devriendt, J., Guiderdoni, B., & Blaizot, J. 2006, *MNRAS*, 370, 1651
- Chabrier, G. 2003, *PASP*, 115, 763
- Cimatti, A., et al. 2004, *Nature*, 430, 184
- Cimatti, A., et al. 2008, *A&A*, 482, 21
- Cirasuolo, M., et al. 2007, *MNRAS*, 380, 585
- Cohen, J. G. 2001, *AJ*, 121, 2895
- Cohen, J. G., Hogg, D. W., Blandford, R., Cowie, L. L., Hu, E., Songaila, A., Shopbell, P., & Richberg, K. 2000, *ApJ*, 538, 29
- Cowie, L. L., Songaila, A., Hu, E. M., & Cohen, J. G. 1996, *AJ*, 112, 839
- Cowie, L. L., Barger, A. J., Hu, E. M., Capak, P., & Songaila, A. 2004, *AJ*, 127, 3137
- Daddi, E., Cimatti, A., Renzini, A., Fontana, A., Mignoli, M., Pozzetti, L., Tozzi, P., & Zamorani, G. 2004, *ApJ*, 617, 746
- Daddi, E., et al. 2005, *ApJ*, 626, 680
- Daddi, E., et al. 2007, *ApJ*, 670, 156
- Damjanov, I., et al. 2009, *ApJ*, 695, 101
- Dawson, S., Stern, D., Bunker, A. J., Spinrad, H., & Dey, A. 2001, *AJ*, 122, 598
- Dekel, A., & Birnboim, Y. 2006, *MNRAS*, 368, 2
- Drory, N., et al. 2009, *ApJ*, 707, 1595
- Elbaz, D., et al. 2007, *A&A*, 468, 33
- Faber, S. M., et al. 2007, *ApJ*, 665, 265
- Feulner, G., Goranova, Y., Drory, N., Hopp, U., & Bender, R. 2005, *MNRAS*, 358, L1
- Fontana, A., et al. 2003, *ApJL*, 594, L9
- Fontana, A., et al. 2009, *A&A*, 501, 15
- Foucaud, S., Conselice, C. J., Hartley, W. G., Lane, K. P., Bamford, S. P., Almaini, O., & Bundy, K. 2010, *MNRAS*, 406, 147
- Franx, M., van Dokkum, P. G., Schreiber, N. M. F., Wuyts, S., Labbé, I., & Toft, S. 2008, *ApJ*, 688, 770
- Franzetti, P., et al. 2007, *A&A*, 465, 711
- Giavalisco M., et al., 2004, *ApJ*, 600, L93
- Grazian, A., et al. 2007, *A&A*, 465, 393
- Hartley, W. G., et al. 2008, *MNRAS*, 391, 1301
- Hartley, W. G., et al. 2010, *MNRAS*, 407, 1212
- Heavens, A., Panter, B., Jimenez, R., & Dunlop, J. 2004, *Nature*, 428, 625
- Hopkins, A. M., & Beacom, J. F. 2006, *ApJ*, 651, 142
- Ichikawa T., et al., 2006, in *Proc. of SPIE*, Vol. 6269, 38
- Ichikawa, T., et al. 2007, *PASJ*, 59, 1081
- Ilbert, O., et al. 2010, *ApJ*, 709, 644
- Jimenez, R., Panter, B., Heavens, A. F., & Verde, L. 2005, *MNRAS*, 356, 495
- Juneau, S., et al. 2005, *ApJL*, 619, L135
- Kajisawa, M., et al. 2006, *PASJ*, 58, 951
- Kajisawa M., Yamada T., 2006, *ApJ*, 650, 12
- Kajisawa, M., et al., 2009, *ApJ*, 702, 1393 (K09)
- Kajisawa, M., Ichikawa, T., Yamada, T., Uchimoto, Y. K., Yoshikawa, T., Akiyama, M., & Onodera, M. 2010, *ApJ*, 723, 129
- Kajisawa, M., et al. 2011, *PASJ*, in press, arXiv:1012.2115
- Kauffmann, G., et al. 2003, *MNRAS*, 341, 54
- Kauffmann, G., Heckman, T. M., De Lucia, G., Brinchmann, J., Charlot, S., Tremonti, C., White, S. D. M., & Brinkmann, J. 2006, *MNRAS*, 367, 1394
- Kriek, M., et al. 2006, *ApJL*, 649, L71
- Kriek, M., van der Wel, A., van Dokkum, P. G., Franx, M., & Illingworth, G. D. 2008, *ApJ*, 682, 896
- Kriek, M., van Dokkum, P. G., Labbé, I., Franx, M., Illingworth, G. D., Marchesini, D., & Quadri, R. F. 2009, *ApJ*, 700, 221
- Longhetti, M., et al. 2007, *MNRAS*, 374, 614
- McCracken, H. J., Ilbert, O., Mellier, Y., Bertin, E., Guzzo, L., Arnouts, S., Le Fèvre, O., & Zamorani, G. 2008, *A&A*, 479, 321
- Moster, B. P., Somerville, R. S., Newman, J. A., & Rix, H.-W. 2010, arXiv:1001.1737
- Nardini, E., Risaliti, G., Salvati, M., Sani, E., Imanishi, M., Marconi, A., & Maiolino, R. 2008, *MNRAS*, 385, L130
- Onodera, M., et al. 2010, *ApJL*, 715, L6
- Pannella, M., et al. 2009, *ApJL*, 698, L116
- Papovich, C., et al. 2007, *ApJ*, 668, 45
- Peng, Y.-j., et al. 2010, *ApJ*, 721, 193
- Pozzetti, L., et al. 2010, *A&A*, 523, A13
- Reddy, N. A., Steidel, C. C., Erb, D. K., Shapley, A. E., & Pettini, M. 2006a, *ApJ*, 653, 1004
- Ryan, R. E., Jr., et al. 2010, arXiv:1007.1460
- Salimbeni, S., et al. 2008, *A&A*, 477, 763
- Salpeter, E. E. 1955, *ApJ*, 121, 161
- Sandage, A., Tammann, G. A., & Yahil, A. 1979, *ApJ*, 232, 352
- Saracco, P., et al. 2005, *MNRAS*, 357, L40
- Schechter, P. 1976, *ApJ*, 203, 297
- Stetson, P. B. 1987, *PASP*, 99, 191
- Suzuki, R., et al. 2008, *PASJ*, 60, 1347
- Treu, T., Ellis, R. S., Liao, T. X., & van Dokkum, P. G. 2005, *ApJL*, 622, L5
- van Dokkum, P. G., et al. 2008, *ApJL*, 677, L5
- Vergani, D., et al. 2008, *A&A*, 487, 89
- Wake, D. A., et al. 2010, arXiv:1012.1317
- Weiner, B. J., et al. 2005, *ApJ*, 620, 595
- Whitaker, K. E., et al. 2010, *ApJ*, 719, 1715
- Wilkins, S. M., Trentham, N., & Hopkins, A. M. 2008, *MNRAS*, 385, 687
- Williams, R. J., Quadri, R. F., Franx, M., van Dokkum, P., & Labbé, I. 2009, *ApJ*, 691, 1879
- Williams, R. J., Quadri, R. F., Franx, M., van Dokkum, P., Toft, S., Kriek, M., & Labbé, I. 2010, *ApJ*, 713, 738
- Wirth, G. D., et al. 2004, *AJ*, 127, 3121
- Yamada, T., et al. 2009, *ApJ*, 699, 1354
- Yoshikawa, T., et al. 2010, *ApJ*, 718, 112
- Zehavi, I., et al. 2005, *ApJ*, 630, 1
- Zirm, A. W., et al. 2007, *ApJ*, 656, 66
- Zucca, E., et al. 2006, *A&A*, 455, 879